Original Research *Highlight article*

Transmembrane serine protease 2 cleaves nidogen 1 and inhibits extrahepatic liver cancer cell migration and invasion

Yong-Biao Ma[1,2]*, Jian-Wen Qiao[3]* and Xiao Hu[4]

[1]Department of Hepatobiliary Surgery, Weifang People's Hospital, Weifang 261041, China; [2]Department of Hepatobiliary Surgery, Shandong Provincial Hospital, Shandong University, Jinan 250021, China; [3]Department of Hepatobiliary Surgery, Weihai Municipal Hospital, Cheeloo College of Medicine, Shandong University, Weihai 264200, China; [4]Department of Hepatobiliary Pancreatic Surgery, The Affiliated Hospital of Qingdao University, Qingdao 266003, China
*These authors contributed equally to this paper.
Corresponding author: Xiao Hu. Email: huxiao202@163.com

Impact statement

This study confirmed that transmembrane serine protease 2 (TMPRSS2) regulates Nidogen 1 (NID1) expression in extracellular vesicles (EVs) and metastatic hepatocellular carcinoma (HCC) cells. It found that TMPRSS2 expression was inversely correlated with the metastatic potential of HCC cell lines. TMPRSS2 overexpression in MHCCLM3 and MHCC97L cells led to the significant downregulation of NID1 expression in total cell lysates and isolated EVs. In contrast, TMPRSS2 silencing resulted in the elevation of NID1 expression in cells and EVs. Also, EVs derived from MHCCLM3 and MHCC97L cells with overexpressed or depleted TMPRSS2 deactivated or activated fibroblasts, respectively. These findings indicated that targeting or activating TMPRSS2 to block communications mediated by EVs between cancer cells and the target tissue microenvironment could offset malignant HCC phenotypes.

Abstract

We aimed to confirm whether transmembrane serine protease 2 (TMPRSS2) regulates nidogen 1 (NID1) expression in extracellular vesicles (EVs) and metastatic hepatocellular carcinoma (HCC) cells. HCC cells, HUVEC cells, MRC-5 cells, HLE cells, MHCCLM3 cells, MHCC97L cells, H2P cells, H2M cells, as well as LO2 cells were cultured according to providers' instruction and EV models were established by using BALB/cAnN-nu mice to facilitate the verifications. We found that TMPRSS2 expression was inversely correlated with the metastatic potential of HCC cell lines. The expression of TMPRSS2 decreased in a time-dependent manner in tumor-bearing model mice implanted with MHCCLM3 cells compared with uninoculated mice. TMPRSS2 overexpression in MHCCLM3 and MHCC97L cells led to the significant downregulation of NID1 expression in total cell lysates and isolated EVs. In contrast, TMPRSS2 silencing resulted in the elevation of NID1 expression in cells and EVs. Administration of EVs from MHCCLM3 and MHCC97L cells with overexpressed or silenced TMPRSS2 inhibited or strengthened, respectively, the invasion, proliferation, and migration of LO2 tumor cells. EVs derived from MHCCLM3 and MHCC97L cells with overexpressed or depleted TMPRSS2 also deactivated or activated fibroblasts, respectively. These EVs secrete inflammatory cytokines and phosphorylated p65, facilitate the colonization of fibroblasts, and augment fibroblast growth and motility. These findings provide evidence for a new candidate drug targeting tumorigenic EV-NID1 to treat HCC.

Keywords: Extrahepatic metastasis, HCC, TMPRSS2, NID1, EV, mice

***Experimental Biology and Medicine* 2023; 248: 91–105. DOI: 10.1177/15353702221134111**

Introduction

Hepatocellular carcinoma (HCC) generally invades the lungs, and lung metastasis is a primary cause of cancer-associated death.[1,2] The involved processes are multifactorial and driven by intercellular communication between various types of cells, including tumor and stromal cells, in the tumor microenvironment.[3,4] Components of the tumor microenvironment have recently been targeted to combat tumor metastasis.[5,6] Cancer-associated fibroblasts (CAFs) are the most abundant and active subset of fibroblasts in the tumor stroma and are crucial for promoting tumor metastasis and progression.[7,8] They are thought to express IL-1β, IL-6, IL-8, TGF-β, CXCL12, collagen, and several pro-inflammatory genes, thereby regulating the inflammatory microenvironment.[7–10] Their interactions with tumor cells have been extensively studied.[11,12] The growth and spread of HCC can be significantly reduced by blocking interactions between cancer cells and CAFs,[13] but the mechanism through which tumor cells are activated to become fibroblasts as well as the pathway through which liver cancer metastasizes to the lung remain unclear.

Functional oncogenes transported via tumor-derived exosomes can mediate remote signal transmission from

distant tumor and local cells, thus affecting the signaling and behavior of recipient cells.[14,15] Evidence based on diverse cancer models has shown that the role of tumor-derived exosomes in generating a pre-metastatic niche is beneficial to the viability of disseminated tumor cells in distant organs.[16] A tumor-supportive microenvironment contributes to the induction of CAF phenotypes in stromal cells through extracellular vesicles (EVs) released from chronic lymphocytic leukemia cells.[17] EVs derived from pancreatic ductal adenocarcinoma initiate the formation of a pre-metastatic niche in naïve mice, thus increasing the burden of liver metastasis.[18] Highly metastatic EVs released from melanoma can be upregulated by mesenchymal–epithelial transition (MET) to become bone marrow progenitor cells and induce vascular leakage at pre-metastatic sites.[19] The above-mentioned previous studies focused on the multiple roles of tumor-derived EVs in modulating the tissue microenvironment to promote metastasis.

Nidogen combines with type IV collagen and laminin to form a ternary complex that connects the two networks and stabilizes the three-dimensional structure of the basement membrane.[20] Therefore, in addition to contributing to the construction and maintenance of the basement membrane and tissue structure, nidogens also reciprocate with cell receptor molecules to control cell migration, polarization, and invasion. This is particularly true for nidogen-1 (NID1), which interacts with the β1 integrin receptor family and αvβ3 integrins.[21,22] Interactions between cells and the basement membrane regulate many cell processes, such as differentiation, proliferation, and apoptosis. Nidogens and leukocyte reactive integrins also act upon each other, promoting neutrophil chemotaxis during inflammation. Interactions between cells and the basement membrane play a role in regulating differentiation, proliferation, apoptosis, and many other cellular processes. Nidogen 1 is abundantly expressed and detectable in the peripheral blood of patients with ovarian cancer.[23] The NID1 promoter is ectopically downregulated in human gastrointestinal cancers.[24] NID1 functions in tumor cell metastasis in patients with breast, melanotic, and endometrial cancers.[25–27] Metastatic HCC cell-derived EVs are rich in NID1, which enhances angiogenesis and pulmonary endothelial permeability, thereby facilitating the formation of a pre-metastatic niche, further contributing to the colonization and extrahepatic metastasis of tumor cells. Clinical findings have shown that serum EV-NID1 level positively correlates with tumor stage.[28]

The membrane-anchored serine protease, transmembrane serine protease 2 (TMPRSS2, a member of the mannan-binding lectin serine protease family),[29] is predominantly expressed in the prostate.[30] The 5′-untranslated region of TMPRSS2 is fused with the E26 transformation-specific (ETS) transcription factors, ERG and ETV1, in prostate cancer tissues.[31] The level of TMPRSS2 protein is related to the progression of prostate cancer,[32,33] and TMPRSS2 induces prostate cancer cells to invade via NID1 degradation.[34] However, the role and interaction of TMPRSS2 with NID1 in HCC metastasis remain obscure.

The most prevalent histological type of primary liver cancer is HCC, which is the third leading cause of cancer-related deaths worldwide. Metastasis is a crucial event in the late stages of hepatocarcinogenesis. The lungs are the most prevalent sites of extrahepatic HCC metastases, which are found in approximately 50% of patients upon presentation.[35] Although a facilitative role of EV-NID1 has been indicated in extrahepatic metastasis of HCC to the lung, the mechanism through which NID1 is regulated in metastatic HCC cells remains unknown. Here, we aimed to confirm whether TMPRSS2 regulates NID1 expression in EVs and metastatic HCC cells. Furthermore, we sought to determine how TMPRSS2 influences HCC cell-derived EVs to promote metastasis and activate lung fibroblasts to create a supportive microenvironment for extrahepatic metastasis.

Materials and methods

Cell culture

Human HCC cell lines (Hep3B and PLC/PRF/5), a human umbilical vein endothelial cell (HUVEC) line, and human lung fibroblasts (MRC-5) were obtained from the American Type Culture Collection (ATCC) and cultured as described by the ATCC.

The HCC epithelial-like cell line (HLE) was obtained from the Japanese Collection of Research Bioresources (JCRB). MHCCLM3 and MHCC97L cells were procured from Fudan University Cancer Institute, and H2P and H2M cells were obtained from Xin-Yuan Guan, University of Hong Kong.[36] The immortalized normal human hepatic cell line, LO2, was provided by the Wuhan Institute of Virology, Chinese Academy of Sciences (Wuhan, China). All cells were cultured in DMEM-F12 medium supplemented with 10% fetal bovine serum (FBS, ScienCell, California, USA), 100 U/mL penicillin, and 100 U/mL streptomycin (ThermoFisher, Massachusetts, USA) at 37 °C with 5% CO_2 and routinely tested to prevent mycoplasma contamination.

Animal experiments

The Committee for the Use of Live Animals in Teaching and Research at the Affiliated Hospital of Qingdao University approved the animal experiments. The study methodologies and all experiments do conform to the Declaration of Helsinki. BALB/cAnN-nu mice were raised in a specific pathogen-free environment in the Laboratory Animal Unit.

Mouse EV models

Briefly, 6-week-old BALB/cAnN-nu male mice received weekly intravenous injections of EVs (15 μg) or PBS (control) for 3 weeks; then, they were transplanted with an orthotopic liver. Four-week-old BALB/cAnN-nu male mice were inoculated with luciferase-labeled MHCCLM3 cells (1×10^6) in the right flank to obtain tumor seeds for orthotopic liver implantation. The harvested tumor pieces were sectioned into ~ 1 mm^3 cubes. The livers of another X anesthetized mice were exposed via laparotomy and implanted with tumor seeds. Tumor development was monitored in mice injected with D-luciferin (Gold Biotechnology Inc., St. Louis MO, USA) weekly by measuring bioluminescence signals using an IVIS® Spectral Imaging System (PerkinElmer Life and Analytical Sciences Inc., Waltham, MA, USA). At the completion of the experiment, the mice were euthanized by

cervical dislocation at 0.5–1 min after intravenous injection of Barbital (100 mg/kg).

Overexpression and knockdown of TMPRSS2 in cells

We transfected pcDNA3.1 vectors (25 μg) carrying the TMPRSS2 coding sequence or pcDNA3.1 empty vectors into MHCCLM3 and MHCC97-L cells (5×10^6/mL) to assess TMPRSS2 overexpression and depletion. We knocked down TMPRSS2 by transfecting 15 μg of siRNA-TMPRSS2 or siRNA-NC into MHCCLM3 and MHCC97L cells (5×10^6/mL). All cells were lysed 48 h later.

Isolation of EVs

The cells were maintained in a medium containing 10% EV-depleted FBS, which was prepared by overnight centrifugation at 100,000 × *g* and 4°C using an Avanti JXN-30 high-speed centrifuge (Beckman Coulter, Inc. Brea, CA, USA). The cells were incubated for 72 h, following which the supernatant was extracted, and EVs were purified through differential centrifugation. Cell debris and dead cells were removed from the supernatant by centrifugation at 2000 × *g* for 15 min using a Heraeus Multifuge X3FR (Thermo Fisher Scientific Inc., Waltham, MA, USA). Microvesicles were centrifuged using Avanti JXN-30 at 20,000 × *g* and 4°C for 30 min and then removed. Supernatants were passed through a Millipore filter (pore size, 0.22 μm) and then centrifuged again at 100,000 × *g* and 4°C for 2 h to obtain EVs. Ultracentrifugation was repeated in the same manner to collect EVs after they were rinsed with PBS.

Blood samples were obtained from the hearts of mice at the end of the experiments, from individuals without liver-related diseases conditions, and from patients with HCC. Circulating EVs were collected from the serum separated from blood samples by centrifugation at 1500 × *g* for 30 min using a Multifuge X3R refrigerated centrifuge (Thermo Scientific Inc.). The circulating EVs were then purified using ExoQuick PLUS Exosome Purification Kits for Serum & Plasma (System Biosciences LLC., Palo Alto, CA, USA) as described by the manufacturer. Large vesicles were precipitated from serum samples by centrifugation at 16,500 × *g* for 45 min using an Eppendorf® Centrifuge 5430R (Eppendorf AG., Hamburg, Germany). Proteins isolated from the EVs were then verified by immunoblotting using anti-α-tubulin, anti-Alix, anti-TSG101, anti-CD9, anti-GM130, and anti-p62 antibodies.

Incubation of LO2 and MRC-5 cells with EVs

We incubated LO2 (1×10^5/well) and MRC-5 (2×10^5/well) cells with 10 μg of EVs in six-well plates for 72 h. The cells were then rinsed twice with PBS, seeded in complete medium for 72 h, and then assayed as described below.

Colony formation assays

The growth of MHCCLM3 or MHCC97L cells incubated under various conditions was assessed as colony formation. Briefly, untreated cells seeded at a density of 1×10^3/well onto 35 mm Petri dishes were cultured overnight at 37°C and then exposed to different conditions for 48 h. Next, the medium was replaced with the current medium and the cells were cultured for 14 days. Colonies were fixed with 4% paraformaldehyde, stained with 0.1% crystal violet, and counted using a microscope at 200× magnification.

CCK-8 assay

Cell viability was assessed using CCK-8 assays, as described by the manufacturer. Cells in 96-well plates were incubated with CCK-8 (10 μL/well) at 37°C for 2 h. The optical density (OD) was then measured at 450 nm using an Infinite M200 microplate reader (Tecan Group AG., Männedorf, Switzerland).

Migration and invasion assays

Migration and invasion were assayed using Transwell® Permeable Supports (Corning Inc., Corning, NY, USA). Transwell® inserts were coated with BD Matrigel™ Basement Membrane Matrix (Becton Dickinson and Co., Franklin Lakes, NJ, USA) invasion assays, following which 5×10^4 cells were resuspended in serum-free medium and seeded onto the upper Transwell® chambers for both assays. Medium supplemented with 10% FBS was added to the lower chamber as a chemotactic agent. After incubation for a predetermined period, cells that passed through the Transwell® membrane were immobilized before staining with crystal violet. Migrating and invading cells were counted in four randomly selected domains.

Quantitative real-time PCR

Total RNA was isolated from cells or tissues using RNeasy Mini Kits (Qiagen GmbH, Hilden, Germany), as described by the manufacturer. The isolated RNA was reverse transcribed by real-time PCR using SuperScript™ VILO™ cDNA Synthesis Kits (Thermo Fisher Scientific Inc.), SYBR™ Green PCR Master Mix (Thermo Fisher Scientific Inc.), and the Applied Biosystems® 7500 Fast Real-Time PCR System (Applied Biosystems, Waltham, MA, USA). All analyses were conducted in triplicate, and hypoxanthine guanine phosphoribosyl transferase I (HPRT) was the reference gene to normalize cytokine expression in different samples. Cytokine expression was determined as copy numbers per HPRT.

Western blotting

Protein contents of whole-cell lysates in RIPA buffer with 1% NP-40, 50 mM Tris-HCl, 150 mM NaCl, and 0.1 % sodium dodecyl sulfate (SDS) were determined using the bicinchoninic acid method. Proteins were separated by 10% SDS–PAGE, blotted onto 0.45 μm polyvinylidene difluoride (PVDF) membranes (Millipore Sigma Co., Ltd., Burlington, MA, USA). Nonspecific protein binding was blocked by incubating the membranes with 5% BSA at 25°C for 1 h. Next, the membranes were incubated overnight with primary antibodies at 4°C, followed by the corresponding secondary antibodies at 25°C for 1 h. Immunoreactivity was calculated using SuperSignal™ West Femto Maximum Sensitivity Substrate Kits (Thermo Fisher Scientific Inc.) and visualized using a C-DiGit® Western Blot Scanner (LI-COR Biosciences, Lincoln, NE, USA).

Statistical analysis

All data were assessed using Predictive Analytics Software PASW Version 18.0 (SPSS Inc., Chicago, IL, USA). Normally distributed data were analyzed using one-way analysis of variance (ANOVA), nonparametric variables were assessed by Mann–Whitney U tests, and non-parametric variables were assessed post hoc by multiple between-group comparisons. Statistical significance was set at $p < 0.05$.

Results

Low expression of TMPRSS2 in HCC cells with metastatic inclination and advanced stage of orthotopic transplantation in mice

At first, to address the role of TMPRESS in HCC metastasis, we examined its expression in HCC samples ($n = 20$) and normal hepatic tissue ($n = 6$). The data indicated that TMPRSS2 was downregulated in HCC samples, compared with normal hepatic tissue (Supplementary Figure 1). We evaluated the role of TMPRSS2 in extrahepatic HCC metastasis as well as the underlying mechanism by comparing TMPRSS2 expression in HCC cells with high metastatic inclination and low metastatic capacity.[28] Both cell lines were engineered with samples from metastatic lesions of patients with HCC and lung metastases.[37] TMPRSS2 expression at the mRNA and protein levels was significantly lower in H2M, HMCCLM3, and HMCC97L cells than in the HCC cell lines with low metastatic inclination, including MIHA and Hep3B cells (Figure 1(A) and (B)). Next, we used an orthotopic liver implantation mouse model to mimic the metastasis progression of HCC, as reported by Mao *et al*.[28] Blood was collected from mice before and after orthotopic liver implantation of luciferase-labeled MHCC97L tumor seed to examine the expression TMPRSS. The expression of TMPRSS2 decreased in a time-dependent manner in tumor samples after HCC tumor seeds were implanted in the liver (Figure 1(C) and (D)). These results suggest that low TMPRSS2 expression is prerequisite for the high metastatic potential of HCC cells.

Expression of TMPRSS2 is correlated inversely with NID1 protein level in cells and isolated EVs

TMPRSS2 causes NID1 degradation in prostate cancer cells.[34] We further explored the correlation between TMPRSS2 and NID1 protein expression in HMCCLM3 and MHCC97L cells. TMPRSS2 and NID1 protein levels were determined in total lysates of cells transfected with the TMPRSS2 overexpression vector. Western blotting showed that the upregulation of TMPRSS2 expression caused a marked time-dependent decline in NID1 expression in cell lysates (Figure 2(A) and (B)). Western blot analysis of siRNA-transfected HMCCLM3 and MHCC97L cells confirmed TMPRSS2 knockdown and increased NID1 protein levels (Figure 2(C) and (D)). These data suggested that TMPRSS2 induced NID1 degradation in these HCC cell lines through direct interaction with NID1.

Next, we examined whether NID1 expression in EVs derived from MHCCLM3 and MHCC97L cells is also downregulated by TMPRSS2. We isolated EVs from MHCCLM3 and MHCC97L cells with TMPRSS2 overexpression or silencing. Positive Alix and TSG101 expression and negative GM130 and p62 expression in EV extracts confirmed that EVs had been isolated from the microenvironment of HCC cells (Figure 3(A)). Western blotting also showed that NID1 expression was higher than that of TMPRSS2 in EVs. The overexpression of TMPRSS2 in both cell lines resulted in a significant downregulation of NID1 expression in EVs compared with cells transfected with the empty vector (oeNC) and untreated cells (Figure 3(B)). In contrast, silencing TMPRSS2 resulted in increased NID1 levels in EVs (Figure 3(B)). These data suggested that TMPRSS2 levels inversely correlate with EV-NID1 levels.

TMPRSS2 dysregulation influences EV-induced hyperproliferation and metastasis of native LO2 liver cells

We investigated the role and mechanism of TMPRSS2 in terms of facilitating the effects of EVs secreted from MHCCLM3 and MHCC97L cells on the malignant properties of native LO2 liver cells. We incubated LO2 cells with EVs from MHCCLM3 and MHCC97L cells with overexpressed or knocked down TMPRSS2. Rates of colony formation and proliferation were markedly increased in LO2 cells incubated with metastatic EVs than in those not incubated with metastatic EVs (Figure 4(A) to (D)). However, EVs derived from TMPRSS2-overexpressing MHCCLM3 and MHCC97L cells ameliorated the growth and proliferation of LO2 cells compared with the controls (Figure 4(A) to (D)). Notably, EVs derived from MHCCLM3 and MHCC97L cells depleted of TMPRSS2 further augmented the number of colonies and proliferation of LO2 cells compared with the controls (Figure 4(A) to (D)).

We examined the involvement of EVs in LO2 cell migration and invasion using Transwell® assays with or without Matrigel membranes. EVs derived from non-transfected HCC cells elevated the migratory and invasive capacity of LO2 cells compared with the cells without EVs (Figure 5(A) to (D)). Moreover, the migration and invasion efficiency was lower in LO2 cells incubated with EVs derived from TMPRSS2-overexpressing MHCCLM3 and MHCC97L cells than in the controls (Figure 5(A) to (D)). Conversely, EVs originating from cells with silenced TMPRSS2 caused more migration and invasion of LO2 cells than the EVs derived from HCC cells transfected with siRNA-NC (Figure 5(A) to (D)). These findings suggest that EVs from highly metastatic HCC cells confer malignant properties to native liver cells and that this phenomenon is associated with low TMPRSS2 expression, probably by regulating NID1 levels in EVs.

Involvement of TMPRSS2 in the activation of pulmonary fibroblasts

Preparing a favorable microenvironment with other cell types recruited for disseminated metastatic cells at distant sites to survive and grow is a sign of a pre-metastatic niche.[25] We co-incubated MRC5 lung fibroblasts with EVs derived from MHCCLM3 and MHCC97L cells. We then analyzed mRNA levels of interleukin 8 (IL-8), IL-6, and IL-1β in MRC5 cells because cytokines are important modulators of cell-cell signaling and they regulate the tumor microenvironment.[38]

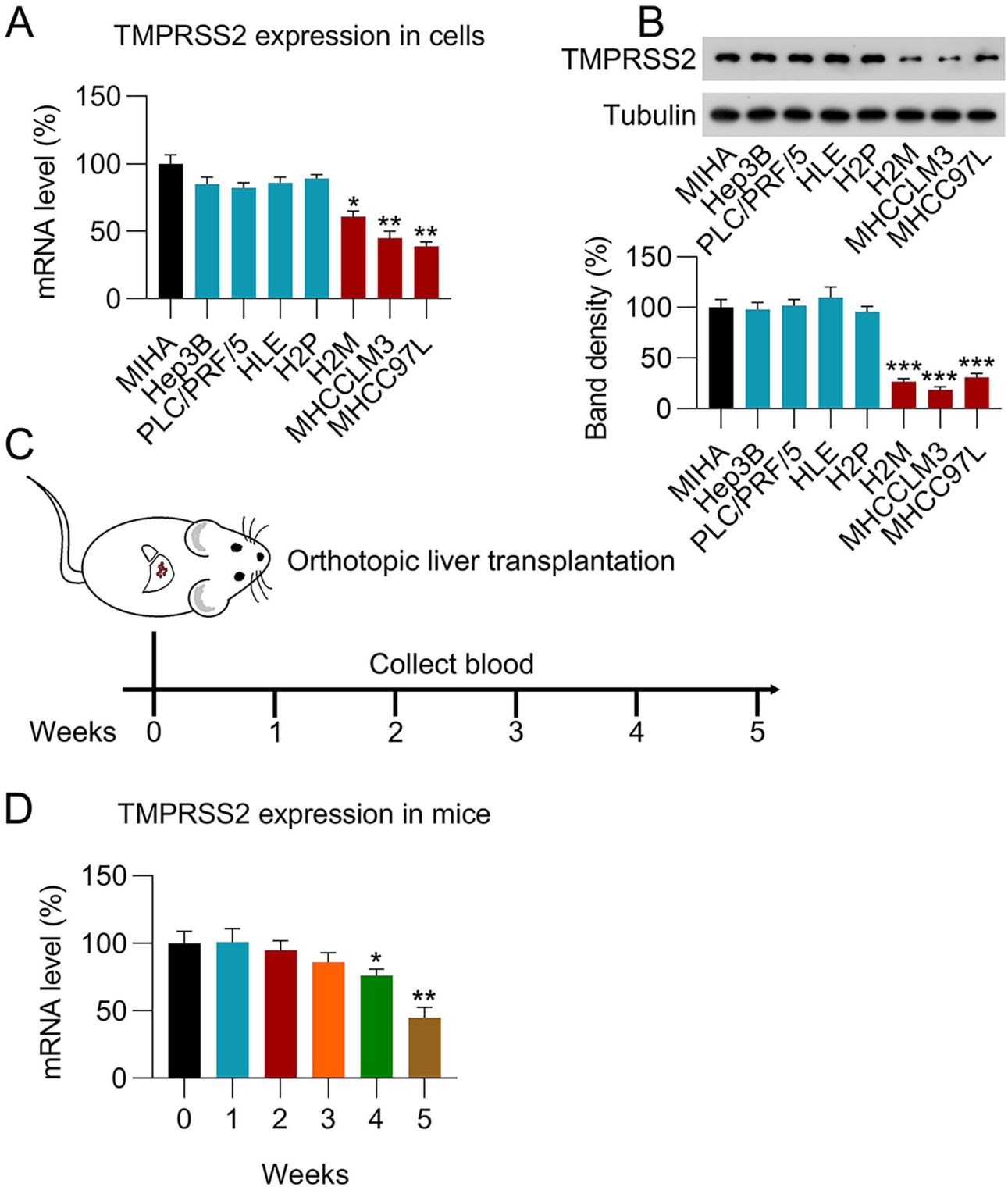

Figure 1. TMPRSS2 levels in highly metastatic HCC cells. (A, B) Real-time PCR and western blotting of TMPRSS2 levels in multiple HCC cell lines. (C, D) Collection of blood from mice before and after implanting MHCCLM3 tumor seeds in orthotopic liver ($n = 3$). mRNA extracted from blood was assessed using real-time PCR. *$p < 0.05$ and **$p < 0.01$ versus the normoxia group. *$p < 0.05$ and **$p < 0.01$ versus indicated group.

EVs from non-transfected HCC cells induced the generation of pro-inflammatory cytokines in MRC5 cells compared with untreated MRC5 cells (Figure 6(A) to (F)). Cytokine production was alleviated when cells were incubated with EVs from cells overexpressing TMPRSS2 (Figure 6(A) to (F)), whereas EVs from cells with silenced TMPRSS2 further upregulated the expression of cytokines compared with the respective controls (Figure 6(A) to (F)).

Upregulated α-SMA levels[39] and phosphorylated NF-κB p65[16] are indicators of fibroblast activation. Therefore, we assessed α-SMA expression and p65 phosphorylation in MRC5 cells after incubation with EVs. Western

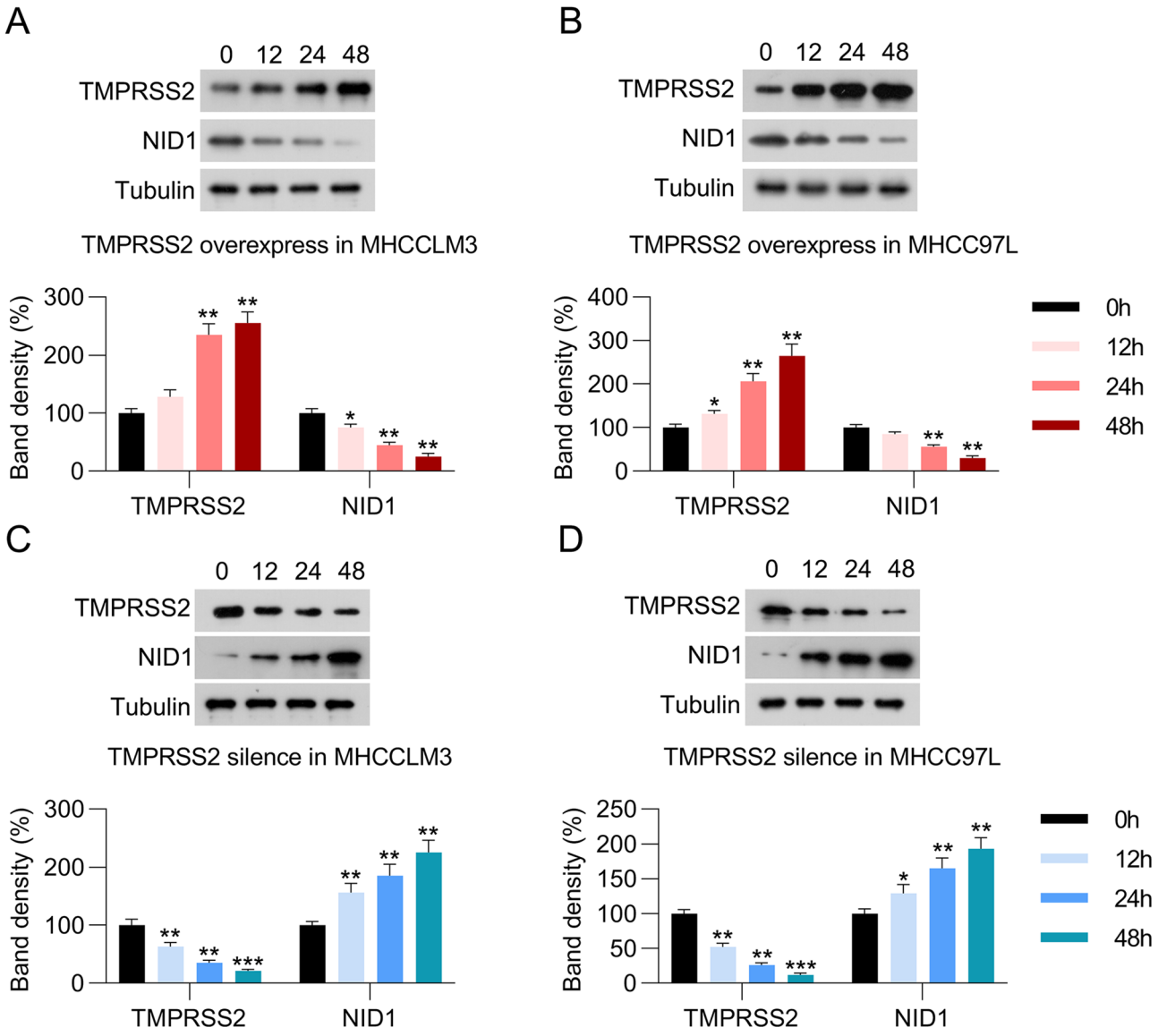

Figure 2. Influence of TMPRSS2 on NID1 expression in MHCCLM3 and MHCC97L cells. We transfected MHCCLM3 and MHCC97L cells with pcDNA3-TMPRSS2 or siRNA-TMPRSS2 (A, B) and then examined the expression profiles of TMPRSS2 and NID1 proteins using western blotting (C, D). $^{*}p < 0.05$, $^{**}p < 0.01$, $^{***}p < 0.001$ versus indicated group.

blotting showed that incubating MRC5 cells with EVs from untreated MHCCLM3 and MHCC97L cells led to increased α-SMA expression and p65 phosphorylation compared with untreated MRC5 cells (Figure 6(G) and (H)). Furthermore, EVs from HCC cells with TMPRSS2 overexpression abolished α-SMA upregulation and p65 phosphorylation (Figure 6(G) and (H)), whereas those from cells with TMPRSS2 depletion upregulated α-SMA expression and increased phosphorylated p65 levels compared with the respective controls (Figure 6(G) and (H)).

The results of colony formation and CCK-8 assays indicated that EVs from HCC cells promoted MRC5 fibroblast colony formation and proliferation rates (Figure 7(A) to (D)), and those from HCC cells overexpressing TMPRSS2 abolished the enhanced proliferation of MRC5 fibroblasts (Figure 7(A) to (D)). However, EVs derived from cells with silenced TMPRSS2 augmented the proliferation of MRC5 fibroblasts promoted by EVs (Figure 7(A) to (D)).

The Transwell® assay results indicated that EVs from untreated HCC cells increased MRC5 migration and invasion compared with untreated MRC5 fibroblasts (Figure 8(A) to (D)). The EVs derived from MHCCLM3 and MHCC97L cells overexpressing TMPRSS2 decreased the migratory and invasion efficiency of MRC5 fibroblasts, whereas those derived from HCC cells with TMPRSS knockdown further enhanced the migration and invasion of MRC5 fibroblasts (Figure 8(A) to (D)). These results indicated that highly metastatic EVs contribute to fibroblast activation and that TMPRSS2 participates in this process by mediating NID1 expression.

TMPRSS2 participates in the generation of metastatic HCC EVs

An EV mouse model[18] was established by repeated EV injections followed by HCC tumor seed implantation into the liver (Figure 9(A)). We collected blood sample from

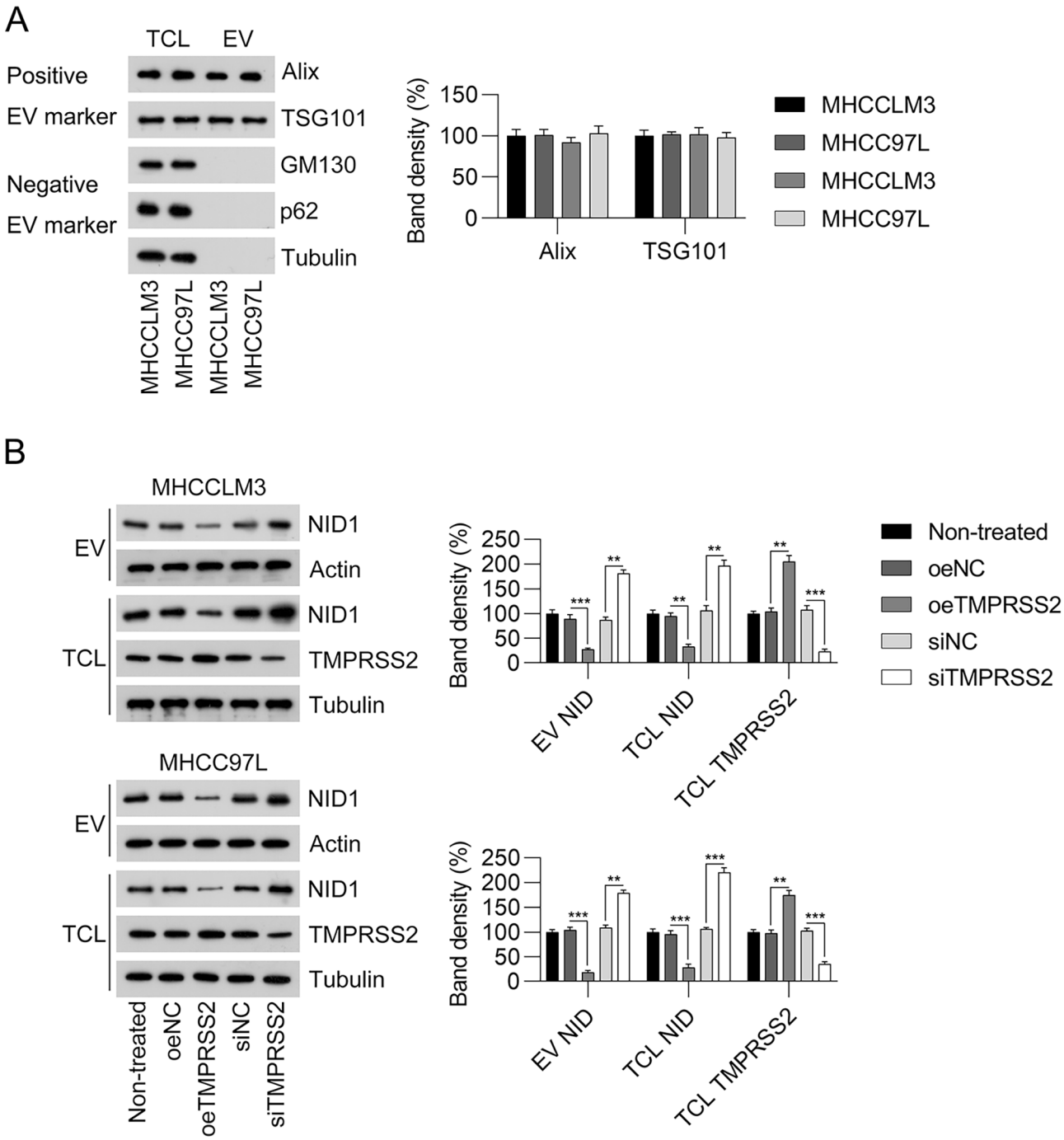

Figure 3. Levels of NID1 in EVs from MHCCLM3 and MHCC97L cells with TMPRSS2 overexpression or depletion. (A) Western blots of EV molecular markers in isolated EVs and total cell lysates (TCL). Positive EV indicators: Alix and TSG101. Negative indicators: cis-Golgi marker GM130, nucleoporin p62 and cytoskeletal α-tubulin. (B) Western blots of TMPRSS2 and NID1 in EVs and TCL.

EV-injected mice at week 0, 1, 3, and 5 post transplantation. mRNA level of TMPRSS2 was gradually reduced in PBS group; injection of non-treated EV and siTMPRSS2-EV caused a robust decline of TMPRSS2 in serum of mice; while siTMPRSS2-EV injection led to a stable and sustained mRNA level of TMPRSS2 (Figure 9(B)). Compared with mice injected with PBS, those with MHCCLM3 cell-derived EVs showed enhanced primary tumor growth in the liver and upregulated distant metastasis to the lung tissues (Figure 9(C) and (D)). However, injecting tumor-bearing mice with EVs from MHCCLM3 cells overexpressing TMPRSS2 resulted in a reduced tumor growth rate in the liver and decreased number of distant lung metastases (Figure 9(C) and (D)). In contrast, injections of EVs derived from MHCCLM3 cells with silenced TMPRSS2 resulted in increased liver tumor growth and bioluminescence in the lung tissue compared with EVs derived from MHCCLM3 cells (Figure 9(C) and (D)). Furthermore, HE staining was performed to examine the status of lung metastasis. It was displayed that injections of EVs derived from MHCCLM3 cells resulted in lung

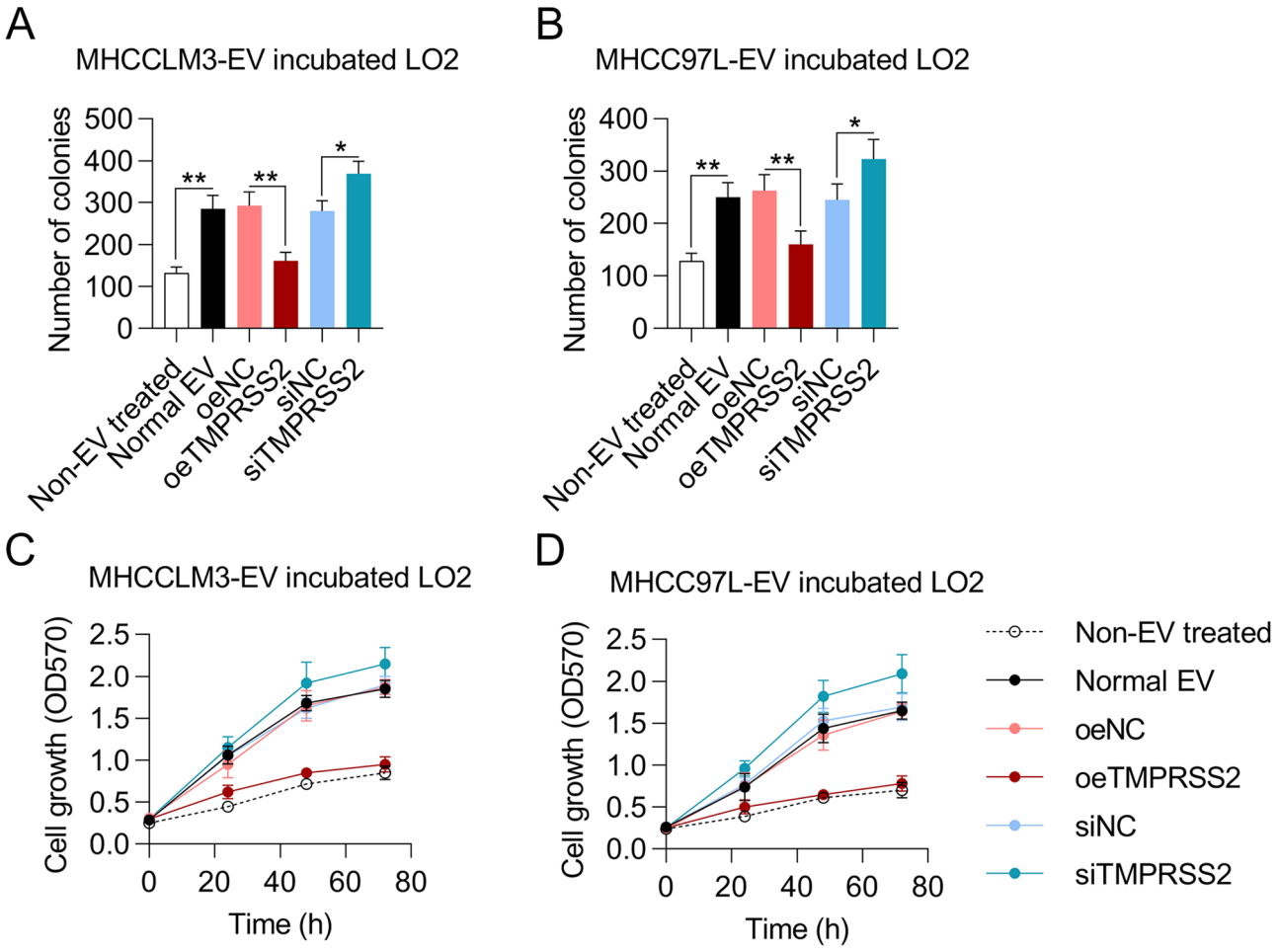

Figure 4. Effects of TMPRSS2 on EVs from MHCCLM3 and MHCC97L cells facilitate LO2 proliferation. (A, B) LO2 cells were incubated with EVs derived from MHCCLM3 or MHCC97L cells with TMPRSS2 depletion or overexpression. Next, colony formation was assayed. Representative images show fixed and crystalline violet-stained colonies. (C, D) Viability of LO2 cells incubated with EVs derived from MHCCLM3 or MHCC97L cells with TMPRSS2 overexpression or depletion determined by CCK-8 assays at various time points. *$p < 0.05$, **$p < 0.01$ versus indicated group.

metastasis. TMPRSS2 overexpression caused a decreased number of distant lung metastases, while its silencing led to moderate metastasis. In addition, we also examined the expression of VEGF, which is a biomarker for HCC metastasis in blood sample from mice. Compared with PBS administration group, non-treated EV and siTMPRSS2-EV injection resulted in higher VEGF level in serum, while oeTMPRSS2-EV injection caused a downregulated serum VEGF mRNA level (Supplementary Figure 2). These data suggested that EVs secreted from HCC cells overexpressing TMPRSS2 inhibited the carcinogenesis of liver tumors and metastasis from distant sites to the lung, whereas silencing TMPRSS2 promoted these properties.

Discussion

The tumor microenvironment serves as a dynamic system regulated by intercellular communication, and it is linked to tumor development and metastasis. Therefore, the relationship between tumor and exosome-mediated stroma requires investigation. We initially compared TMPRSS2 expression profiles between highly metastatic HCC and normal cells and found that TMPRSS2 expression was downregulated in the former. We further revealed that TMPRSS2 caused NID1 degradation in both MHCCLM3 and MHCC97L cells and their secreted EVs. The EVs from TMPRSS2-overexpressing or -silenced MHCCLM3 and MHCC97L cells were directly transferred from tumor cells to native LO2 liver cells and MRC5 fibroblasts. EVs from cells overexpressing TMPRSS2 led to a decrease in the number of malignant phenotypes of liver cells and fibroblast deactivation, whereas EVs from cells with TMPRSS2 depletion conferred metastasis and proliferation capacity to LO2 and MRC5 cells. In addition, EVs from MHCCLM3 cells promoted tumor development and extrahepatic metastasis to the lung, whereas this phenomenon was alleviated and augmented by TMPRSS2 overexpression and silencing, respectively. The crosstalk between tumor cell and fibroblast EVs clarified the molecular mechanism of HCC cell invasion as well as the reasons why liver cancer is highly invasive. This has significant implications for effective prevention and treatment strategies.

Components of EVs were transferred to adjacent and distant cells to complete the mediation of intercellular communication by EVs. The uptake of oncogenic EV content resulted in increased aggressiveness of recipient cells. EVs derived from HCC tumors promote the migration and

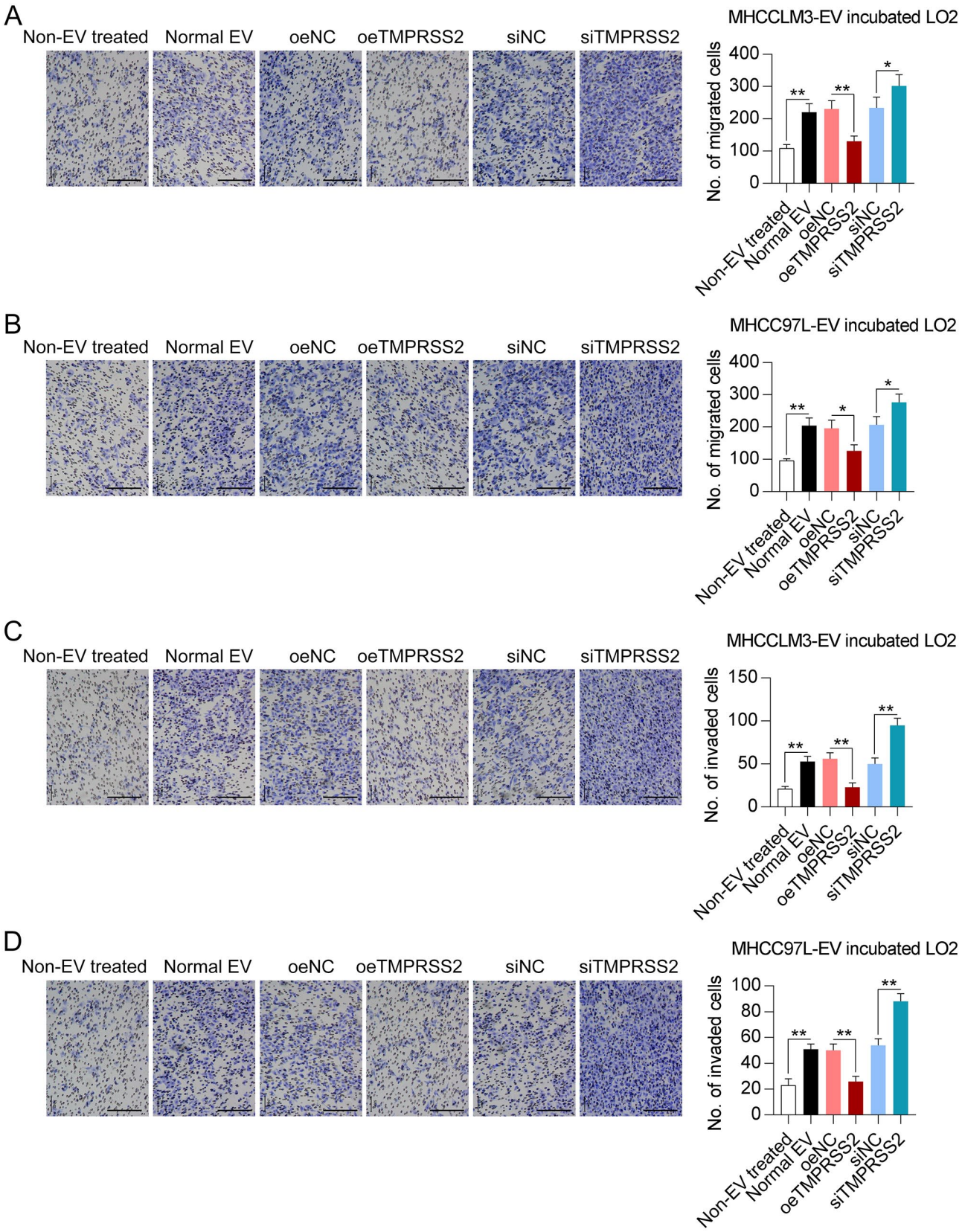

Figure 5. Involvement of TMPRSS2 in MHCCLM3 and MHCC97L cell-derived EVs facilitated LO2 cell migration and invasion. (A, B) Assays were conducted to investigate migration and (C, D) invasion of LO2 cells pretreated with EVs derived from MHCCLM3 or MHCC97L cells with TMPRSS2 overexpression or depletion. Control cells were cultured with PBS. Representative images show fixed and crystalline violet-stained migrating and invading cells at the conclusion of experiment. Scale bar, 100 μm. *$p < 0.05$, **$p < 0.01$ versus indicated group.

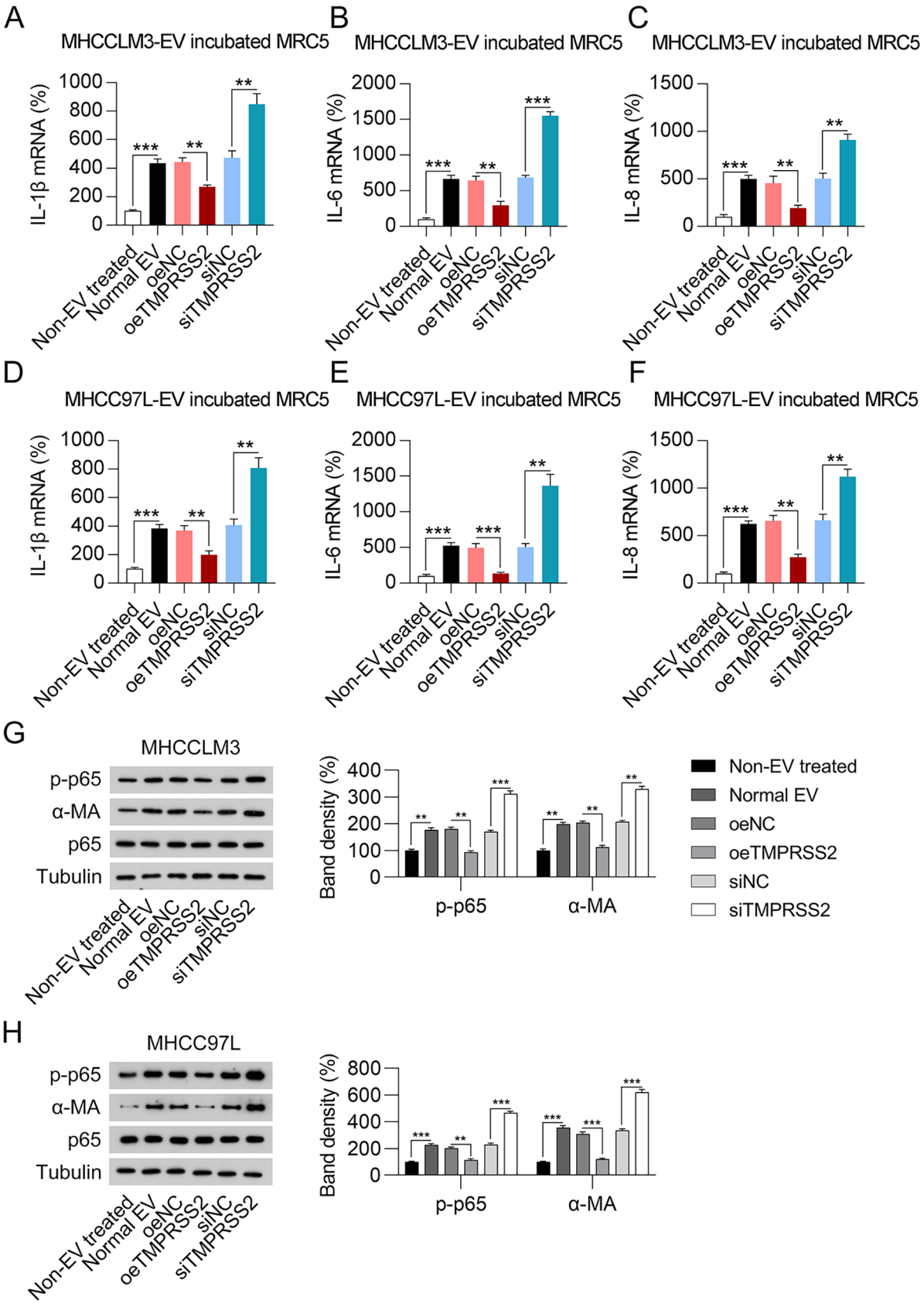

Figure 6. Effects of EVs derived from MHCCLM3 and MHCC97L cells with TMPRSS2 overexpression or depletion on MRC5 fibroblast proliferation. Relative mRNA levels of (A, D) IL-1β, (B, E) IL-6, and (C, F) IL-8 in MRC5 cells incubated with EVs derived from MHCCLM3 or MHCC97L cells with TMPRSS2 overexpression or depletion determined by real-time PCR. (G, H) Western blots of α-MA expression and p65 phosphorylation in MRC5 cells incubated with EVs derived from MHCCLM3 or MHCC97L cells with TMPRSS2 overexpression or depletion. $^{**}p < 0.01$, $^{***}p < 0.001$ versus indicated group.

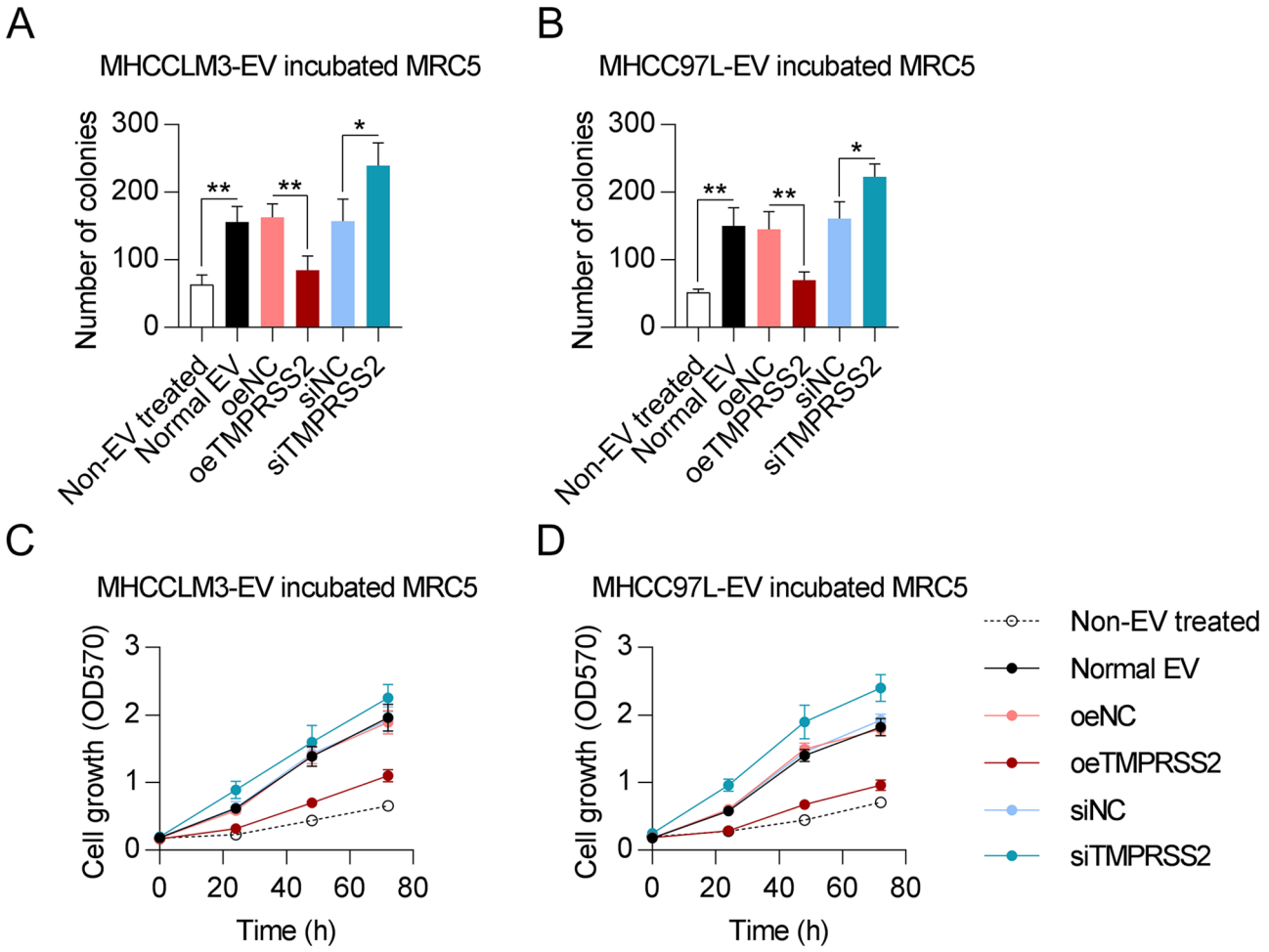

Figure 7. Effects of EVs derived from MHCCLM3 and MHCC97L cells with TMPRSS2 overexpression or depletion on the proliferation of MRC5 fibroblasts. (A, B) MRC5 cells were incubated with EVs derived from MHCCLM3 or MHCC97L cells, following which colony formation was quantified. Representative images show fixed and crystalline violet-stained colonies. (C, D) CCK-8 assay results at different time points of MRC5 cells incubated with EVs derived from MHCCLM3 or MHCC97L cells with TMPRSS2 overexpression or depletion. $^{*}p < 0.05$, $^{**}p < 0.01$ versus indicated group.

invasion of immortalized hepatocytes[40] and the epithelial–mesenchymal transition (EMT) to trigger cancer progression.[41] For instance, transferring miRNAs from HCC-derived EVs to recipient cells facilitates the formation of new vasculature,[42] cell movement,[43] vasopermeability,[44] and multidrug resistance,[45] while activating cell signaling.[14] In fact, with the overexpression or knockdown of TMPRSS2, an inducer of NID1,[34] HCC cells secreted EVs with different NID1 expression profiles, suggesting that EV components could be regulated via cellular interaction. Our *in vivo* findings indicated that EVs released from HCC cells play crucial roles in the development of cancer and extrahepatic metastasis to the lungs. Gain-and-loss-of-function experiments further indicated that EVs derived from MHCCLM3 cells overexpressing TMPRSS2 improved the efficiency of tumor development and metastasis, whereas EVs from MHCCLM3 cells with silenced TMPRSS2 fostered tumor formation and lung metastasis. Mao *et al*. linked these findings to NID1 levels in EVs.[28] Their findings showed that EVs with high NID1 levels promoted the extrahepatic metastasis of liver cancer by activating pulmonary fibroblasts. The present findings were consistent with these.

Cell invasion is promoted by the removal of basement membranes[46] and is regulated during angiogenesis, organogenesis, and trophoblast implantation.[47] During tumorigenesis, malignant tumors are characterized by invasion via the basement membrane, the integrity of which is destroyed, generating an environment that allows invasion that might contribute to the proliferation and invasion of cancer cells.[48] NID1 is prevalent as a connector among laminins, collagens, and proteoglycans in the extracellular matrix and basement membranes beneath the epithelia of most major organ systems.[49] NID1 combines with cell surface integrins, participates in the establishment and maintenance of basement membranes and tissue architecture, acts reciprocally with cell receptor molecules, and modulates cell migration, invasion, and polarization.[50] Therefore, we speculated that NID1 dysregulation contributes to the accelerated metastatic capacity of tumor cells. To the best of our knowledge, this is the first study to report that TMPRSS2 promotes NID1 degradation in HCC cell lines. With the upregulation of TMPRSS2, NID1 levels in cells and EVs were gradually reduced, whereas TMPRSS2 depletion led to high levels of NID1 at the cellular and EV levels. We did not find TMPRSS2 in EVs derived from

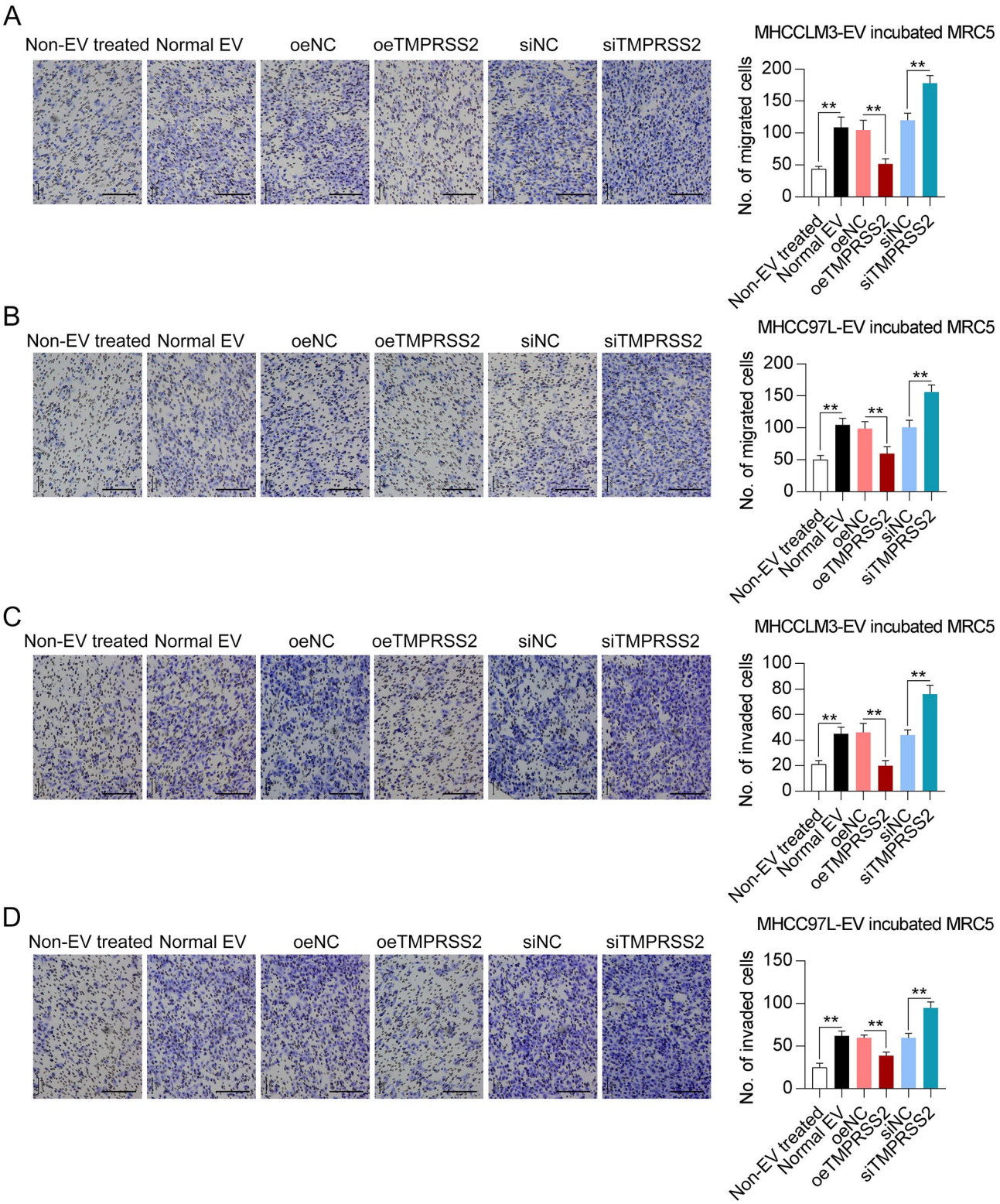

Figure 8. Effects of EVs derived from MHCCLM3 and MHCC97L cells with TMPRSS2 overexpression or depletion on migration and invasion of MRC5 fibroblasts. (A, B) Migration and (C, D) invasion of MRC5 fibroblasts incubated with EVs derived from MHCCLM3 or MHCC97L cells with TMPRSS2 overexpression or depletion. Controls were incubated with PBS. Images are representative of fixed and crystalline violet-stained migrating and invading cells at the conclusion of experiment. Scale bar, 100 μm. $^{**}p < 0.01$, $^{***}p < 0.001$ versus indicated group.

MHCCLM3 and MHCC97L cells. Therefore, NID1 might act as a bridge that promotes the influence of TMPRSS2 on tumor cells and fibroblasts.

Collectively, our findings indicated the functional and clinical significance of TMPRSS2 in HCC and showed that targeting or activating TMPRSS2 to block communications

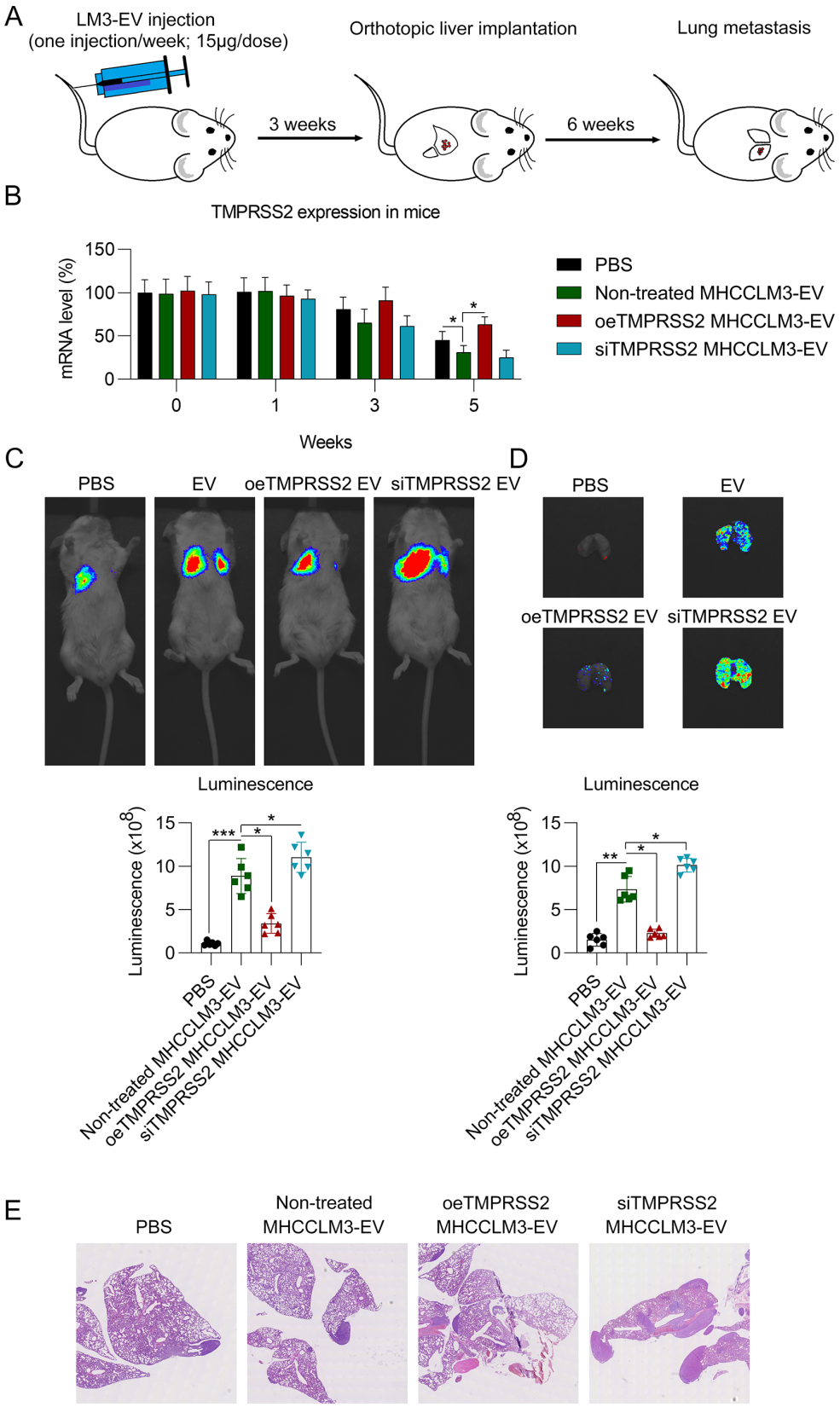

Figure 9. Influence of EVs derived from MHCCLM3 cells with TMPRSS2 dysregulation promoted HCC tumorigenesis and metastasis. (A) Sketch of EV mouse model. Tail veins of nude mice were injected weekly with EVs (15 μg per week) derived from MHCCLM3 cells for 3 weeks before orthotopic liver implantation of tumor seeds derived from luciferase-labeled MHCCLM3 cells ($n = 3$). Analysis of liver tumors and distant lung metastases 5 weeks thereafter. (B) Collection of blood from mice before and after implanting MHCCLM3 tumor seeds in orthotopic liver. TMPRSS2 mRNA extracted from blood were assessed using real-time PCR. (C) Quantification of luciferase bioluminescence in mice at the conclusion of experiment. (D) Luciferase bioluminescence quantified in dissected lung tissues. (E) HE staining was utilized to show the distant lung metastases. *$p < 0.05$, **$p < 0.01$, ***$p < 0.001$ versus indicated group.

mediated by EVs between cancer cells and the target tissue microenvironment could offset malignant HCC phenotypes.

AUTHORS' CONTRIBUTIONS

All authors participated in the design, interpretation of the studies and analysis of the data, and review of the article; YBM, JWQ, and XH conducted the experiments; YBM and JWQ wrote the article.

DECLARATION OF CONFLICTING INTERESTS

The author(s) declared no potential conflicts of interest with respect to the research, authorship, and/or publication of this article.

FUNDING

The author(s) received no financial support for the research, authorship, and/or publication of this article.

ORCID ID

Xiao Hu https://orcid.org/0000-0002-1959-9178

SUPPLEMENTAL MATERIAL

Supplemental material for this article is available online.

REFERENCES

1. Uka K, Aikata H, Takaki S, Shirakawa H, Jeong SC, Yamashina K, Hiramatsu A, Kodama H, Takahashi S, Chayama K. Clinical features and prognosis of patients with extrahepatic metastases from hepatocellular carcinoma. *World J Gastroenterol* 2007;**13**:414
2. Wang H, Chen L. Tumor microenviroment and hepatocellular carcinoma metastasis. *J Gastroenterol Hepatol* 2013;**28**:43–8
3. Hanahan D, Weinberg RA. Hallmarks of cancer: the next generation. *Cell* 2011;**144**:646–74
4. Quail DF, Joyce JA. Microenvironmental regulation of tumor progression and metastasis. *Nat Med* 2013;**19**:1423–37
5. Fang H, DeClerck YA. Targeting the tumor microenvironment: from understanding pathways to effective clinical trials. *Cancer Res* 2013;**73**:4965–77
6. Sounni NE, Noel A. Targeting the tumor microenvironment for cancer therapy. *Clin Chem* 2013;**59**:85–93
7. Kalluri R, Zeisberg M. Fibroblasts in cancer. *Nat Rev Cancer* 2006;**6**:392–401
8. Kalluri R. The biology and function of fibroblasts in cancer. *Nat Rev Cancer* 2016;**16**:582–98
9. Erez N, Truitt M, Olson P, Hanahan D. Cancer-associated fibroblasts are activated in incipient neoplasia to orchestrate tumor-promoting inflammation in an NF-κB-dependent manner. *Cancer Cell* 2010;**17**:135–47
10. Sharon Y, Raz Y, Cohen N, Ben-Shmuel A, Schwartz H, Geiger T, Erez N. Tumor-derived osteopontin reprograms normal mammary fibroblasts to promote inflammation and tumor growth in breast cancer. *Cancer Res* 2015;**75**:963–73
11. Räsänen K, Vaheri A. Activation of fibroblasts in cancer stroma. *Exp Cell Res* 2010;**316**:2713–22
12. Jung DW, Che ZM, Kim J, Kim K, Kim KY, Williams D, Kim J. Tumor-stromal crosstalk in invasion of oral squamous cell carcinoma: a pivotal role of CCL7. *Int J Cancer* 2010;**127**:332–44
13. Mazzocca A, Fransvea E, Dituri F, Lupo L, Antonaci S, Giannelli G. Down-regulation of connective tissue growth factor by inhibition of transforming growth factor β blocks the tumor–stroma cross-talk and tumor progression in hepatocellular carcinoma. *Hepatology* 2010;**51**:523–34
14. Kogure T, Lin WL, Yan IK, Braconi C, Patel T. Intercellular nanovesicle-mediated microRNA transfer: a mechanism of environmental modulation of hepatocellular cancer cell growth. *Hepatology* 2011;**54**:1237–48
15. Al-Nedawi K, Meehan B, Micallef J, Lhotak V, May L, Guha A, Rak J. Intercellular transfer of the oncogenic receptor EGFRvIII by microvesicles derived from tumour cells. *Nat Cell Biol* 2008;**10**:619–24
16. Fang T, Lv H, Lv G, Li T, Wang C, Han Q, Yu L, Su B, Guo L, Huang S. Tumor-derived exosomal miR-1247-3p induces cancer-associated fibroblast activation to foster lung metastasis of liver cancer. *Nat Commun* 2018;**9**:1–13
17. Paggetti J, Haderk F, Seiffert M, Janji B, Distler U, Ammerlaan W, Kim YJ, Adam J, Lichter P, Solary E. Exosomes released by chronic lymphocytic leukemia cells induce the transition of stromal cells into cancer-associated fibroblasts. *Blood* 2015;**126**:1106–17
18. Costa-Silva B, Aiello NM, Ocean AJ, Singh S, Zhang H, Thakur BK, Becker A, Hoshino A, Mark MT, Molina H, Xiang J, Zhang T, Theilen TM, García-Santos G, Williams C, Ararso Y, Huang Y, Rodrigues G, Shen TL, Labori KJ, Lothe IM, Kure EH, Hernandez J, Doussot A, Ebbesen SH, Grandgenett PM, Hollingsworth MA, Jain M, Mallya K, Batra SK, Jarnagin WR, Schwartz RE, Matei I, Peinado H, Stanger BZ, Bromberg J, Lyden D. Pancreatic cancer exosomes initiate pre-metastatic niche formation in the liver. *Nat Cell Biol* 2015;**17**:816–26
19. Peinado H, Alečković M, Lavotshkin S, Matei I, Costa-Silva B, Moreno-Bueno G, Hergueta -Redondo M, Williams C, García-Santos G, Ghajar CM. Melanoma exosomes educate bone marrow progenitor cells toward a pro-metastatic phenotype through MET. *Nat Med* 2012;**18**:883–91
20. Timpl R, Brown JC. Supramolecular assembly of basement membranes. *Bioessays* 1996;**18**:123–32
21. Dedhar S, Jewell K, Rojiani M, Gray V. The receptor for the basement membrane glycoprotein entactin is the integrin alpha 3/beta 1. *J Biol Chem* 1992;**267**:18908–14
22. Yi XY, Wayner EA, Kim Y, Fish AJ. Adhesion of cultured human kidney mesangial cells to native entactin: role of integrin receptors. *Cell Adhes Commun* 1998;**5**:237–48
23. Li L, Zhang Y, Li N, Feng L, Yao H, Zhang R, Li B, Li X, Han N, Gao Y, Xiao T, Wu L. Nidogen-1: a candidate biomarker for ovarian serous cancer. *Jpn J Clin Oncol* 2015;**45**:176–82
24. Ulazzi L, Sabbioni S, Miotto E, Veronese A, Angusti A, Gafà R, Manfredini S, Farinati F, Sasaki T, Lanza G. Nidogen 1 and 2 gene promoters are aberrantly methylated in human gastrointestinal cancer. *Mol Cancer* 2007;**6**:1–9
25. Zhou Y, Zhu Y, Fan X, Zhang C, Wang Y, Zhang L, Zhang H, Wen T, Zhang K, Huo X. NID1, a new regulator of EMT required for metastasis and chemoresistance of ovarian cancer cells. *Oncotarget* 2017;**8**:33110
26. Pedrola N, Devis L, Llauradó M, Campoy I, Martinez-Garcia E, Garcia M, Muinelo-Romay L, Alonso-Alconada L, Abal M, Alameda F, Mancebo G, Carreras R, Castellví J, Cabrera S, Gil-Moreno A, Matias-Guiu X, Iovanna JL, Colas E, Reventós J, Ruiz A. Nidogen 1 and Nuclear Protein 1: novel targets of ETV5 transcription factor involved in endometrial cancer invasion. *Clin Exp Metastasis* 2015;**32**:467–78
27. Alečković M, Wei Y, LeRoy G, Sidoli S, Liu DD, Garcia BA, Kang Y. Identification of Nidogen 1 as a lung metastasis protein through secretome analysis. *Genes Develop* 2017;**31**:1439–55
28. Mao X, Tey SK, Yeung CLS, Kwong EML, Fung YME, Chung CYS, Mak LY, Wong DKH, Yuen MF, Ho JCM, Pang H, Wong MP, Leung CO, Lee TKW, Ma V, Cho WC, Cao P, Xu X, Gao Y, Yam JWP. Nidogen 1-enriched extracellular vesicles facilitate extrahepatic metastasis of liver cancer by activating pulmonary fibroblasts to secrete tumor necrosis factor receptor 1. *Adv Sci* 2020;**7**:2002157
29. Paoloni-Giacobino A, Chen H, Peitsch MC, Rossier C, Antonarakis SE. Cloning of the TMPRSS2 gene, which encodes a novel serine protease with transmembrane, LDLRA, and SRCR domains and maps to 21q22. *3. Genomics* 1997;**44**:309–20
30. Lin B, Ferguson C, White JT, Wang S, Vessella R, True LD, Hood L, Nelson PS. Prostate-localized and androgen-regulated expression of the membrane-bound serine protease TMPRSS2. *Cancer Res* 1999;**59**:4180–4
31. Tomlins SA, Rhodes DR, Perner S, Dhanasekaran SM, Mehra R, Sun X-W, Varambally S, Cao X, Tchinda J, Kuefer R. Recurrent fusion of TMPRSS2 and ETS transcription factor genes in prostate cancer. *Science* 2005;**310**:644–8

32. Lucas JM, True L, Hawley S, Matsumura M, Morrissey C, Vessella R, Nelson PS. The androgen-regulated type II serine protease TMPRSS2 is differentially expressed and mislocalized in prostate adenocarcinoma. *J Pathol* 2008;**215**:118–25
33. Chen YW, Lee MS, Lucht A, Chou FP, Huang W, Havighurst TC, Kim K, Wang JK, Antalis TM, Johnson MD, Lin CY. TMPRSS2, a serine protease expressed in the prostate on the apical surface of luminal epithelial cells and released into semen in prostasomes, is misregulated in prostate cancer cells. *Am J Pathol* 2010;**176**:2986–96
34. Ko C-J, Huang C-C, Lin H-Y, Juan C-P, Lan S-W, Shyu H-Y, Wu S-R, Hsiao P-W, Huang H-P, Shun C-T. Androgen-induced TMPRSS2 activates matriptase and promotes extracellular matrix degradation, prostate cancer cell invasion, tumor growth, and metastasis. *Cancer Res* 2015;**75**:2949–60
35. Duseja A. Staging of hepatocellular carcinoma. *J Clin Exp Hepatol* 2014; **4**:S74–9
36. Lee TK, Man K, Ho JW, Wang XH, Poon RT, Sun CK, Ng KT, Ng IO, Xu R, Fan ST. Significance of the Rac signaling pathway in HCC cell motility: implications for a new therapeutic target. *Carcinogenesis* 2005;**26**:681–7
37. Li Y, Tang ZY, Ye SL, Liu YK, Chen J, Xue Q, Chen J, Gao DM, Bao WH. Establishment of cell clones with different metastatic potential from the metastatic hepatocellular carcinoma cell line MHCC97. *World J Gastroenterol* 2001;**7**:630–6
38. Kwa MQ, Herum KM, Brakebusch C. Cancer-associated fibroblasts: how do they contribute to metastasis? *Clin Exp Metas* 2019;**36**:71–86
39. Ji J, Eggert T, Budhu A, Forgues M, Takai A, Dang H, Ye Q, Lee JS, Kim JH, Greten TF, Wang XW. Hepatic stellate cell and monocyte interaction contributes to poor prognosis in hepatocellular carcinoma. *Hepatology* 2015;**62**:481–95
40. He M, Qin H, Poon TC, Sze SC, Ding X, Co NN, Ngai SM, Chan TF, Wong N. Hepatocellular carcinoma-derived exosomes promote motility of immortalized hepatocyte through transfer of oncogenic proteins and RNAs. *Carcinogenesis* 2015;**36**:1008–18
41. Chen L, Guo P, He Y, Chen Z, Chen L, Luo Y, Qi L, Liu Y, Wu Q, Cui Y. HCC-derived exosomes elicit HCC progression and recurrence by epithelial-mesenchymal transition through MAPK/ERK signalling pathway. *Cell Death Dis* 2018;**9**:1–17
42. Lin X-J, Fang J-H, Yang X-J, Zhang C, Yuan Y, Zheng L, Zhuang S-M. Hepatocellular carcinoma cell-secreted exosomal microRNA-210 promotes angiogenesis in vitro and in vivo. *Mol Therap: Nucl Acids* 2018; **11**:243–52
43. Liu H, Chen W, Zhi X, Chen EJ, Wei T, Zhang J, Shen J, Hu LQ, Zhao B, Feng XH, Bai XL, Liang TB. Tumor-derived exosomes promote tumor self-seeding in hepatocellular carcinoma by transferring miRNA-25-5p to enhance cell motility. *Oncogene* 2018;**37**:4964–78
44. Fang JH, Zhang ZJ, Shang LR, Luo YW, Lin YF, Yuan Y, Zhuang SM. Hepatoma cell-secreted exosomal microRNA-103 increases vascular permeability and promotes metastasis by targeting junction proteins. *Hepatology* 2018;**68**:1459–75
45. Fu X, Liu M, Qu S, Ma J, Zhang Y, Shi T, Wen H, Yang Y, Wang S, Wang J. Exosomal microRNA-32-5p induces multidrug resistance in hepatocellular carcinoma via the PI3K/Akt pathway. *J Exp Clin Cancer Res* 2018;**37**:52
46. Sherwood DR, Butler JA, Kramer JM, Sternberg PWJC. FOS-1 promotes basement-membrane removal during anchor-cell invasion in C. *Elegans* 2005;**121**:951–62
47. Murray MJ, Lessey BA. Embryo implantation and tumor metastasis: common pathways of invasion and angiogenesis. *Semin Reprod Endocrinol* 1999;**17**:275–90
48. Lester BR, McCarthy JB. Tumor cell adhesion to the extracellular matrix and signal transduction mechanisms implicated in tumor cell motility, invasion and metastasis. *Cancer Metastasis Rev* 1992;**11**: 31–44
49. Miosge N, Holzhausen S, Zelent C, Sprysch P, Herken R. Nidogen-1 and nidogen-2 are found in basement membranes during human embryonic development. *Histochem J* 2001;**33**:523–30
50. Köhling R, Nischt R, Vasudevan A, Ho M, Weiergräber M, Schneider T, Smyth N. Nidogen and nidogen-associated basement membrane proteins and neuronal plasticity. *Neurodegener Dis* 2006;**3**:56–61

(Received May 6, 2022, Accepted September 5, 2022)